Published online May 31, 2005

Nucleic Acids Research, 2005, Vol. 33, No. 10 ***3095–3108***
doi:10.1093/nar/gki611

UNR translation can be driven by an IRES element that is negatively regulated by polypyrimidine tract binding protein

Sigrid Cornelis*, Sandrine A. Tinton, Bert Schepens, Yanik Bruynooghe and Rudi Beyaert

Department for Molecular Biomedical Research, VIB—Ghent University, Unit of Molecular Signal Transduction in Inflammation, B-9052 Gent-Zwijnaarde, Belgium

Received as resubmission May 1, 2005; Accepted May 4, 2005

ABSTRACT

Upstream of N-*ras* (Unr) has been described as an internal initiation *trans*-acting factor (ITAF) in the cap-independent translation of some particular viral and cellular mRNAs. Two factors led us to hypothesize that the UNR 5′-untranslated region (5′-UTR) may contain an internal ribosome entry site (IRES). The first was the requirement for persisting Unr expression under conditions that correlate with cap-independent translation. The other was the observation that the primary UNR transcript contains a 447 nt long 5′-UTR including two upstream AUGs that may restrict translation initiation via cap-dependent ribosome scanning. Here we report that the UNR 5′-UTR allows IRES-dependent translation, as revealed by a dicistronic reporter assay. Various controls ruled out the contribution of leaky scanning, cryptic promoter sequences or RNA processing events to the ability of the UNR 5′-UTR to mediate internal initiation of translation. Ultraviolet cross-linking analysis and RNA affinity chromatography revealed the binding of polypyrimidine tract binding protein (PTB) to the UNR IRES, requiring a pyrimidine-rich region (nucleotides 335–355). Whereas overexpression of PTB in several cell lines inhibited UNR IRES activity and UNR protein expression, depletion of endogenous PTB using RNAi increased UNR IRES activity. Moreover, a mutant version of the UNR IRES lacking the PTB binding site was more efficient at directing IRES-mediated translation. In conclusion, our results demonstrate that translation of the ITAF Unr can itself be regulated by an IRES that is downregulated by PTB.

INTRODUCTION

Translation of eukaryotic mRNAs begins with recruitment of the translation machinery at either the 5′-m^7G cap structure or at an internal ribosome entry site (IRES) [reviewed in (1–3)]. The cap-dependent mechanism for initiating translation is generally thought to be more common; however, the number of mRNAs reported to initiate translation internally is growing, and it is likely that up to 10% of all mRNAs are able to initiate translation by this mechanism (2). Internal initiation seems to facilitate the translation of particular viral and cellular mRNAs under conditions that render the cap-dependent mechanism less efficient, for example under conditions of amino acid starvation (4), cell death (5–8), hypoxia (9,10), heat shock (11) and during the G2/M stage of the cell cycle (7,12–18). Although the mechanism of action of cellular IRESes is currently not understood, it has become clear that some of these elements require auxiliary factors, so-called IRES-*trans*-acting factors (ITAFs), to function. It has been proposed that a major role of ITAFs is to act as RNA chaperones either to maintain or to attain the correct three-dimensional IRES structure that is required for efficient assembly of the 48S complex (19,20).

Upstream of N-*ras* (Unr) is an RNA binding protein that has been identified as an ITAF in IRES-mediated translation of viral and cellular mRNAs (19,21,22). Unr is constituted of five cold-shock domains (CSDs) (23–25), and is a member of the cold-shock family of single-stranded nucleic acid binding proteins (23). The CSD is the most conserved nucleic acid binding sequence, with >40% identity and >60% similarity between bacteria and vertebrates (26–28). In eubacteria, cold-shock proteins consist of one single CSD and are thought to function as RNA chaperones. They have been implicated in various cellular processes, including adaptation to low temperatures, cellular growth and nutrient stress (26,29). In eukaryotic proteins, the CSD is found in combination with several other

*To whom correspondence should be addressed. Tel: +32 9 33 13 600; Fax: +32 9 33 13 609; Email: Sigrid.Cornelis@dmbr.ugent.be
Correspondence may also be addressed to Rudi Beyaert. Tel: +32 9 33 13 600; Fax: +32 9 33 13 609; Email: Rudi.Beyaert@dmbr.ugent.be

types of modules that are thought to confer either a greater specificity of template recognition or an ancillary enzymatic function. Whereas some of these proteins serve as transcription regulators, others have a predominantly cytoplasmic function, influencing the translation state of an mRNA during development and stress responses (26,30,31). In addition, the CSD-related protein, Unr, has been shown to play a role in IRES-dependent translation (19,21,22). Unr stimulates Apaf-1 IRES-dependent translation by acting as an RNA chaperone that, following RNA binding, changes the structure of the Apaf-1 IRES into one that is functionally competent for 48S formation (19). Unr is also required for efficient initiation of translation from the HRV IRES element (21,32) and has been shown to serve as a stimulatory factor in the G2/M-specific regulation of PITSLRE IRES-mediated translation (22).

The 5′-untranslated region (5′-UTR) of UNR is very well conserved among vertebrates, and its unusual length is not very compatible with the cap-dependent scanning mechanism (Figure 1A). The latter observation, and the role of CSD proteins in cellular stress responses, led us to hypothesize that Unr protein expression is regulated by an IRES present in the UNR 5′-UTR. In this study we provide evidence that translation of the mRNA encoding Unr can indeed be initiated by an internal initiation mechanism. In addition we identified polypyrimidine tract binding protein (PTB) as a negative regulator of UNR IRES-dependent translation.

MATERIALS AND METHODS

Plasmid constructs

The human UNR 5′-UTR and the c-*myc* 5′-UTR were isolated by a 5′-RACE reaction on poly(A)$^+$ mRNA from HeLa cells, using the SMART^{TM} RACE cDNA Amplification Kit (Clontech) according to the manufacturer's instructions. The gene-specific primers A + B and C + D (see below) were used to amplify the UNR 5′-UTR and c-*myc* 5′-UTR, respectively. Subsequently, amplification products of 446 nt (for UNR) and 398 nt (for c-*myc*) were cloned in the pT-Advantage vector, according to the instructions of the manufacturer (Clontech). The deletion mutants UNR(1–261), UNR(1–334) and UNR(1–390) were amplified by PCR with primer pairs A + E, A + F and A + G, respectively (see below). The deletion mutant UNRΔ335–355 was constructed by overlap PCR using primers H + I as overlap primers.

The dicistronic pSV-Sport expression vectors (Di-pRF-UNR) containing the different UNR fragments inserted between the *Renilla* (R) (first cistron) and firefly (F) luciferase (luc) (second cistron) genes were obtained by two steps of three-point ligation as follows.

(i) UNR fragments digested with XbaI–NcoI were cloned together with the firefly luciferase gene, obtained as an NcoI–HindIII fragment from pSV-Sport-Fluc, in the XbaI–HindIII linearized vector pUC19.
(ii) The UNR–Fluc inserts were then recovered as XbaI fragments and cloned in the XbaI linearized pSV-Sport-Rluc. The Di-pRF-cMYC expression vector was obtained in a similar way.

The dicistronic pSV-Sport expression vector, Di-pFR-UNR, containing the UNR fragment inserted between the firefly luciferase (first cistron) and *Renilla* luciferase (second cistron) genes was obtained by two steps of three-point ligation as follows.

(i) The UNR fragment digested with XbaI–NcoI was cloned together with the *Renilla* luciferase gene obtained as an NcoI–HindIII fragment from pSV-Sport-Rluc in the XbaI–HindIII linearized pUC19 vector.
(ii) The UNR–Rluc insert was then recovered as an XbaI fragment and cloned in the XbaI linearized pSV-Sport-Fluc.

To insert a stable stem–loop structure ($\Delta G = -56.8$ kcal/mole at 37°C) immediately upstream of the firefly luciferase open reading frame, we performed a PCR on the pGL3-basic plasmid with primers J and K. The resulting amplification product was digested with HindIII–XbaI and subsequently cloned back into pGL3-basic, generating pGL3-basic-hp. A stem–loop structure was created because oligonucleotide J contains 26 terminal nucleotides that are complementary to a 26 bp sequence upstream of the HindIII site in pGL3-basic. The hpFluc fusion was subsequently cloned as a KpnI–XbaI fragment in the pSV-Sport vector, generating pSV-Sport-hpFluc. Di-phpFR-UNR was constructed as described above for constructing Di-pFR-UNR, but using pSV-Sport-hpFluc instead of pSV-Sport-Fluc.

To create the empty dicistronic vector Di-pRF, a DNA fragment containing the firefly luciferase coding region was excised from pSV-sport-Fluc and inserted into the pSV-sport-Rluc downstream of the *Renilla* luciferase coding region at the XbaI site.

The pGL3-UNR construct was obtained by ligating the UNR 5′-UTR as a HindIII–NcoI fragment into the HindIII–NcoI opened pGL3-basic vector.

For the ultraviolet (UV) cross-linking experiments, the different UNR PCR fragments (XbaI–NcoI digested) were cloned into the pUC19 plasmid in which a T7 promoter had been inserted (22).

PTB (a gift from Dr R. Jackson) and PTBΔnls were amplified using primer pairs L + M and N + M, respectively. The resultant amplicons were fused to an E-tag as NotI–XhoI fragments in the pCAGGS expression vector.

The following PCR primers were used: A, 5′-CTAGTCTAGATGCTGCTTATGGCGGCGCTGGAGAGGG-3′; B, 5′-CATGCCATGGCGCAGTGATACTCAAATATTGCACTTTCAGT-3′; C, 5′-CATGTCTAGATAATTCCAGCGAGAGGCAGAGGGAGCG; D, 5′-CATGCCATGGTCGCGGGAGGCTGCTGGTTTTCCAC-3′; E, 5′-CATGCCATGGAAAGACTACTAGCAGCGTTGGGAAGTG-3′; F, 5′-CATGCCATGGTGATCTACCAAGCTAATAAAGAATACAAC-3′; G, 5′-CATGCCATGGAGCACACGTTTCAAAGGATGAAAGTT-3′; H, 5′-CTTTATTAGCTTGGTAGATCATACTAGCAAGTTTCATCCTTTGAAACG-3′; I, 5′-TGATCTACCAAGCTAATAAAGAATAC-3′; J, 5′-CCCAAGCTTACTTAGATCGCAGATCTCGAGCCCGGGAACCATGGAAGACG; CCAAAAACATAAAGAAAGG-3′; K, 5′-CCGACTCTAGAATTACACGGCGATCTT-3′; L, 5′-ATAAGAAAGCGGCCGCTATGGACGGCATTGTCCCAGATATAG-3′; M, 5′-AACCGCTCGAGCTAGATGGTGGACTTGGAGAAGGAGACCCG-3′; N, 5′-ATAAGAAAGCGGCCGCTATGGTCCCCTCTAGAGTGATCCACATCC-3′.

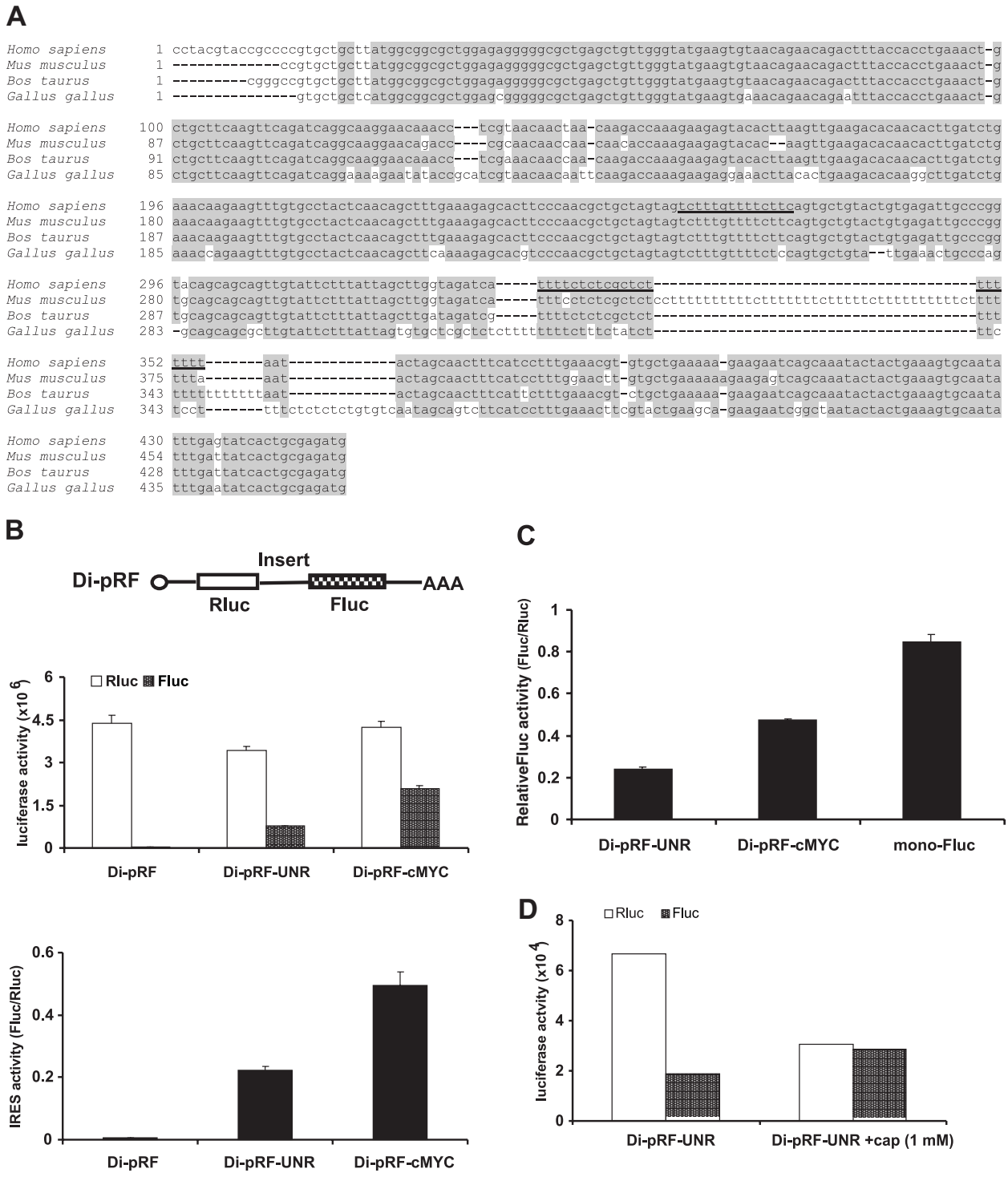

Figure 1. UNR 5′-UTR directs internal ribosome entry. (**A**) Homology between the sequences *Mus musculus*, *Gallus gallus*, *Bos taurus* and human UNR 5′-UTRs. Sequences were aligned from the ATG sequence encoding the initiating methionine. Identical nucleotides in three of the four sequences are indicated by gray boxes. Two pyrimidine-rich sequences are underlined. (**B**) Upper panel: schematic representation of a dicistronic mRNA containing the UNR-specific sequence cloned as an intercistronic sequence between the coding regions for firefly luciferase (Fluc) and *Renilla* luciferase (Rluc). Middle panel: comparison of the IRES activity mediated by the UNR 5′-UTR and the c-*myc* IRES. The dicistronic expression vectors Di-pRF, Di-pRF-UNR and Di-pRF-cMYC were transfected in HEK293T cells, and the activities of Fluc and Rluc were measured after 24 h. The bars represent the average ($n = 3$) ± SD of Fluc (hatched bars) and Rluc (open bars) activities. Lower panel: representation of the IRES activities calculated as the ratio between Fluc and Rluc. (**C**) Comparison of the efficiency of internal initiation mediated by the UNR 5′-UTR to cap-dependent initiation of translation. The dicistronic expression vectors Di-pRF-UNR and Di-pRF-cMYC and a mixture of monocistronic pSV-Sport *Renilla* luciferase and pSV-Sport firefly luciferase plasmids were transfected in HEK293T cells, and the activities of Fluc and Rluc were measured after 24 h. Bars represent the average ($n = 3$) ± SD of the ratio between Fluc and Rluc activities, and are representative of three independent transfection experiments. (**D**) UNR 5′-UTR driven translation of the downstream cistron is not sensitive to cap analogue. *In vitro* synthesized capped transcript derived from Di-pRF-UNR was translated in HeLa S3 cell extract in the absence or presence of 1 mM m^7GpppG cap analogue and Rluc and Fluc activities were measured as described in Materials and Methods.

Transient DNA transfection, RNAi and reporter gene assay

Cells were typically grown in Dulbecco's modified Eagle's medium supplemented with 10% (v/v) heat-inactivated fetal calf serum, 100 U/ml penicillin and 100 μg/ml streptomycin.

Cos-1 cells and Chinese hamster ovary (CHO) cells were transiently transfected using Lipofectamine Plus reagent (Invitrogen) as specified by the manufacturer. Human embryonic kidney HEK293T cells (a gift from Dr M. Hall) were transiently transfected by the calcium phosphate precipitation method (33).

For the RNA interference assays, HEK293T cells were seeded to a density of 5×10^5 cells per well in a 6-well plate on day 1. The following day 200 pmoles of siRNA duplex (Dharmacon) was transfected using Lipofectamine 2000 (Invitrogen) according to the manufacturers' instructions. After 6 h, transfected cells were split into two wells of a 6-well plate. On day 3, cells were retransfected with a mixture of 200 pmoles of siRNA duplex and 750 ng di-pRF-UNR. Later on, transfected cells were again split into three wells of a 6-well plate. 24 and 48 h after the second transfection, cells were harvested for either western blotting or reporter gene assays.

Lysates were prepared from transfected cells using 1× Passive Lysis Buffer (Promega). Both *Renilla* and firefly luciferase activities were measured using the Dual-Luciferase Reporter Assay System (Promega) following the manufacturer's instructions, and light emission was detected by a Topcount scintillation counter (PerkinElmer). Activity of the β-galactosidase transfection control was measured in the presence of chlorophenol red-β-D-galactopyranoside substrate (Roche).

In vitro transcription and translation

The *in vitro* translation assays were performed in HeLa S3 cell extracts prepared according to the protocol described by Bergamini *et al*. (34). Briefly, 80 ng of capped dicistronic transcript was mixed with 4 μl of cell lysate in a final reaction volume of 10 μl containing 16 mM HEPES–KOH (pH 7.6), 20 mM creatine phosphate, 0.1 μg/μl creatine kinase, 0.1 mM spermidine, 100 μM amino acids, 50 mM K-acetate and 2.5 mM Mg-acetate. The translation reactions were carried out at 37°C for 60 min in the absence or in the presence of the cap analogue m^7GpppG (1 mM final concentration) and luciferase activities were measured as described above by using the Dual-Luciferase Reporter Assay System (Promega).

UV cross-linking assays and immunoprecipitation

For UV cross-linking assays, DNA templates for synthesis of the RNA probes were generated by linearizing pUC19 T7 plasmids containing the EMCV IRES, PITSLRE IRES or different fragments of UNR with the appropriate restriction enzymes. Internally labeled RNA probes were synthesized by *in vitro* transcription with T7 polymerase (MAXIscript T7 RNA polymerase kit; Ambion) in the presence of 50 μCi [α-^{32}P]-UTP (Amersham Biosciences).

The cytoplasmic extracts used for the UV cross-linking assays were prepared from HEK293T cells. The cells were collected, washed with cold phosphate-buffered saline (PBS) and recovered by centrifugation at 2500 × *g* for 5 min at 4°C. The cell pellets were resuspended in 100 μl of lysis buffer A containing 10 mM HEPES–KOH (pH 7.4), 3 mM $MgCl_2$, 40 mM KCl, 5% (v/v) glycerol, 1 mM DTT, 0.3% (v/v) Nonidet P40, 200 U/ml aprotinin, 0.1 mM phenylmethylsulfonyl fluoride (PMSF) and 10 μg/ml leupeptin. After lysis, the samples were centrifuged at 20 000 × *g* for 10 min at 4°C. The supernatants were recovered, adjusted to a final protein concentration of 10 mg/ml and kept at −80°C. UV cross-linking assays were performed as described (35). ^{32}P-labeled RNA probes ($\sim 1 \times 10^6$ c.p.m.) were incubated with either 400 ng recombinant PTB (a gift from Dr R. Jackson) or 10 μl cytoplasmic extract (100 μg proteins) for 20 min at 30°C in a 25 μl reaction mixture containing 10 mM HEPES–KOH (pH 7.4), 3 mM $MgCl_2$, 5% (v/v) glycerol, 1 mM DTT, 100 mM KCl, 40 U RNasin (Promega) and 6 μg tRNA. After RNA binding, the reaction mixtures were irradiated on ice with UV light for 30 min using a 'GS gene pulser UV chamber' (Bio-Rad). The samples were then incubated with RNase A and RNase T1 for 60 min at 37°C. The RNA–protein complexes were resolved by 10% SDS–PAGE, the gels were dried and the results were visualized with a Phosphorimager (Molecular Dynamics).

For immunoprecipitation, following RNase cocktail treatment of samples, 1.5 μl of mouse monoclonal anti-E-tag antibody (Amersham Biosciences) was added. After overnight incubation at 4°C on a rotary mixer, 30 μl of protein G-Sepharose beads (Amersham Biosciences), previously equilibrated in lysis buffer A, were added and incubation was continued for 3 h. After washing 6 times with 1 ml buffer containing 50 mM HEPES–KOH (pH 7.4), 250 mM NaCl, 1% (v/v) NP-40, 5 mM EDTA, 200 U/ml aprotinin, 0.1 mM PMSF and 10 μg/ml leupeptin, resin bound proteins were detached from the beads by adding 30 μl of Laemmli sample buffer and heating the mixture for 5 min at 95°C. The proteins were then resolved by 10% SDS–PAGE.

RNA affinity chromatography

Biotinylated RNA probes were synthesized from linearized pUC19 T7 plasmids by *in vitro* transcription with T7 polymerase (MEGAshortscript T7 RNA polymerase kit; Ambion) in the presence of biotinylated CTP (ratio 4 CTP:1 bioCTP) (Pierce). 50 pmol of the biotinylated RNA were incubated with 25 μl streptavidin beads (Pierce) in 200 μl binding buffer containing 20 mM HEPES–KOH (pH 7.4), 50 mM KCl, 5% (v/v) glycerol, 1 mM DTT, 0.5 mM EDTA, 200 U/ml aprotinin, 0.1 mM PMSF, 10 μg/ml leupeptin and 25 μg/ml tRNA. After 1 h at 4°C on a rotary mixer, beads were washed 2 times with binding buffer and added to 20 μl of cytosolic extract (200 μg protein) (prepared as described above) in a total volume of 500 μl, and incubation was continued for 2 h. After washing the beads 3 times with binding buffer and 2 times with binding buffer containing 100 mM KCl, RNA bound proteins were eluted by addition of 200 μl Laemmli sample buffer and analyzed by western blot.

Western blot analysis

Cells were lysed in a buffer containing 20 mM Tris–HCl (pH 8.0), 150 mM NaCl, 10% (v/v) glycerol, 1% (v/v) Nonidet P40, 10 mM EDTA, 200 U/ml aprotinin, 1 mM Pefabloc, 0.1 mM PMSF and 10 μg/ml leupeptin. Equal amounts of

protein were separated by SDS–PAGE and then transferred onto nitrocellulose membrane by electroblotting. The blots were probed with rabbit anti-Unr polyclonal antibody (a kind gift from Dr R. Jackson) diluted 1:4000. Mouse anti-β actin antibody was purchased from ICN Biomedicals. Antibodies against firefly luciferase were obtained from Promega. Anti-PTB antibodies were obtained from Santa Cruz.

Membranes were incubated with horseradish peroxidase-conjugated secondary antibodies against mouse (Amersham Biosciences), rabbit (Amersham Biosciences) or goat (Santa Cruz Biotechnology) immunoglobulin. Proteins were revealed with an enhanced chemiluminescence kit (NEN Renaissance, PerkinElmer).

Cellular RNA purification and northern blotting

Poly(A)$^+$ RNA was isolated from transfected HEK293T cells using the FastTrack® 2.0 mRNA Isolation Kit (Invitrogen) according to the manufacturer's instructions. RNA was denaturated in glyoxal/dimethylsulfoxide, separated on a 1% agarose gel and transferred onto a nylon membrane by a capillary blot procedure. A UV Stratalinker apparatus (Stratagene) was used to cross-link the transferred DNA, and the filters were hybridized with cDNA probes labeled with α-[^{32}P]dCTP by randomly primed DNA synthesis, using the Radprime DNA labeling system kit (Invitrogen). Results were visualized with the Phosphorimager (Molecular Dynamics).

RESULTS

The UNR 5′-UTR directs translation from a dicistronic messenger

To address the possibility that the UNR 5′-UTR directs translation initiation from an internal ribosome entry we created the dicistronic plasmid Di-pRF-UNR by insertion of the UNR 5′-UTR between the two reporter genes, *Renilla* luciferase (Rluc) and firefly luciferase (Fluc), of the empty dicistronic plasmid di-pRF (Figure 1B). Di-pRF, Di-pRF-UNR and Di-pRF-cMYC, which contains the well-characterized cellular c-*myc* IRES, were transfected in HEK293T cells. The Rluc and Fluc activities were determined. A comparison of the downstream cistron activities revealed that both the UNR 5′-UTR and the c-*myc* IRES drastically increased Fluc expression, whereas Rluc activities were comparable (Figure 1B). The extent to which expression of the downstream cistron was enhanced by the UNR 5′-UTR and the c-*myc* IRES differed. In fact, the UNR 5′-UTR and the c-*myc* IRES elevated Fluc activity by ∼40-fold and 100-fold, respectively. To further determine the strength of the putative IRES, UNR 5′-UTR driven internal initiation was also compared with cap-mediated translation. Therefore, monocistronic Fluc and Rluc (to correct for transfection efficiency) constructs were cotransfected and assayed in parallel. As shown in Figure 1C, relative Fluc activity in the mono-Fluc expressing cell lysates was only 5-fold higher than that measured in Di-pRF-UNR transfected cells. This result demonstrates that the UNR 5′-UTR drives translation of a downstream cistron with a 20% efficiency compared with cap-mediated translation. All together, from these results we conclude that internal initiation of translation driven by the UNR 5′-UTR is clearly significant when compared with the potent c-*myc* IRES and with cap-mediated translation.

To further investigate the presence of an IRES in the UNR 5′-UTR, we also synthesized the capped dicistronic transcript Di-pRF-UNR *in vitro* and tested its ability to direct IRES-mediated translation in an *in vitro* translation assay based on HeLa S3 cell extracts. Figure 1D shows that both cistrons are expressed. Moreover, when we artificially inhibited cap-dependent translation by adding m^{7}GpppG cap analogue to the HeLa S3 extracts, translation of only the first cistron was strongly inhibited, whereas expression of the second cistron was even enhanced relative to that seen in the absence of m^{7}GpppG cap analogue. This observation demonstrates that the UNR 5′-UTR drives internal initiation of translation of the downstream cistron independently of the cap-dependent translation of the upstream cistron.

All together, the reported data indicate the presence of an IRES in the UNR 5′-UTR. It should be noted that the ability of the UNR 5′-UTR to support translation of the 3′ cistron does not depend on the arrangement of the reporter genes since no significant difference is observed in the relative expression patterns of the second cistron produced by the dicistronic vectors Di-pFR-UNR and Di-pRF-UNR, respectively (data not shown).

Internal initiation of translation mediated by the UNR 5′-UTR is not due to enhanced ribosomal readthrough, cryptic promoter activity or RNA processing

To further confirm the presence of an IRES in the UNR 5′-UTR and to exclude a possible contribution from cap-dependent mechanisms, e.g. ribosomal readthrough, leaky scanning or ribosome jumping, we generated an additional dicistronic plasmid (Di-phpFR-UNR) that is identical to its parent plasmid (Di-pFR-UNR), with the exception of an inverted repeat inserted immediately upstream of the Fluc coding region. In the mRNA transcribed from this construct, the inverted repeat results in formation of a stable hairpin loop ($\Delta G = -56$ kcal/mole at 37°C). Each of these plasmids was cotransfected with the pSV-Sport β-galactosidase plasmid (used as a transfection control) in HEK293T cells, and cell lysates were assayed for enzymatic activities. As expected, the presence of a stable hairpin loop decreased relative Fluc expression >10-fold indicating that the secondary structure of the hairpin loop blocks cap-dependent ribosome scanning (Figure 2A). Simultaneously, the upstream hairpin loop did not inhibit translation of Rluc. These data further demonstrate that translation of the second cistron is mediated mainly by a cap-independent mechanism.

To exclude the possibility that expression of the second cistron on the dicistronic messenger is derived from a monocistronic RNA, the transcription of which is initiated by putative promoter activity present in the UNR 5′-UTR, we generated pGL3-UNR, in which the UNR 5′-UTR is inserted in the promoterless pGL3-basic vector upstream of the Fluc coding sequence. This plasmid as well as the pGL3-SV40 plasmid (a vector containing the SV40 early promoter and serving as a positive control) and the promoterless pGL3-basic plasmid were cotransfected with pSV-Sport *Renilla* luciferase; the latter was used to correct for variation of transfection efficiency. Figure 2B shows that the relative

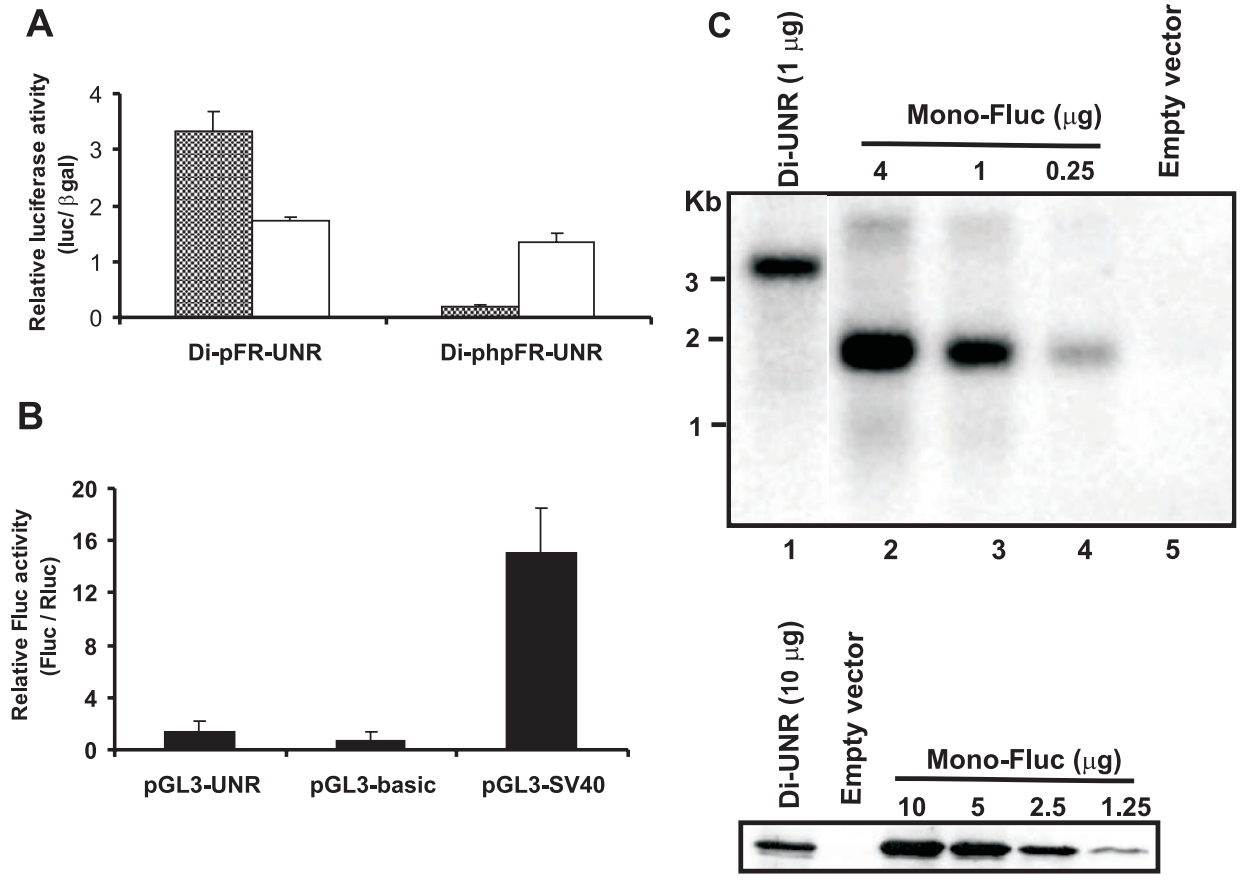

Figure 2. Translation of the second cistron is not due to leaky scanning, readthrough, reinitiation or aberrant mRNA species. (**A**) Influence of a stable hairpin ($\Delta G = -56$ kcal/mol at 37°C) inserted upstream of the first cistron. Dicistronic expression vector Di-pFR-UNR or Di-phpFR-UNR was cotransfected with the pSV-Sport β-galactosidase plasmid in HEK293T cells. Fluc and Rluc activity was normalized to the β-galactosidase activity. The hatched and open bars represent the average ($n = 3$) ± SD of relative Fluc activities and relative Rluc activities, respectively. Bars are representative of three independent transfection experiments. (**B**) Analysis of potential cryptic promoter activity present in the UNR 5′-UTR. pGL3-UNR, pGL3-SV40 and pGL3-basic were cotransfected with the pSV-Sport *Renilla* luciferase plasmid in HEK293T cells. Bars represent the average ($n = 3$) ± SD of the ratio between Fluc and Rluc activities and are representative of three independent transfection experiments. (**C**) The dicistronic expression vector Di-pRF-UNR and a mixture of monocistronic pSV-Sport *Renilla* luciferase and pSV-Sport firefly luciferase plasmids were transfected in HEK293T cells. Poly(A)$^+$ mRNA was isolated as described in Materials and Methods and protein extracts were prepared in parallel. Upper panel: northern blot analysis of a serial dilution (1/4) of poly(A)$^+$ RNA prepared from monocistronic Fluc/Rluc transfectants starting from 4 μg down to 0.25 μg. On the same gel 1 μg poly(A)$^+$ mRNA from dicistronic Di-UNR transfectants was loaded. Dicistronic and monocistronic mRNA expression in the HEK293T transfectants were revealed with a cDNA probe corresponding to the firefly luciferase open reading frame. Numbers on the left indicate the length of RNA markers (New England Biolabs). Lower panel: Fluc protein expression levels of a serial dilution (1/2) starting from 10 μg down to 1.25 μg protein extract from mono-Fluc transfectants. On the same gel a 10 μg cell extract from the Di-pRF-UNR transfectants was loaded.

Fluc activity measured in pGL3-UNR transfected cells is comparable to that measured in cells transfected with the pGL3-basic plasmid, and is ∼15 times lower than the activity produced by pGL3-SV40. This result clearly illustrates that the UNR 5′-UTR is devoid of promoter activity.

To exclude a possible contribution of UNR 5′-UTR-mediated RNA splicing or RNA cleavage to the expression of the second reporter gene, we also examined the integrity of the dicistronic transcripts by northern blot analysis following transfection of HEK293T cells with the Di-pRF-UNR plasmid (Figure 2C, upper panel, lane 1). As a control, we also analyzed in parallel cells expressing monocistronic Fluc mRNA (Figure 2C, upper panel, lanes 2–4). Cells transfected with the empty pSV-Sport plasmid (Figure 2C, lane 5) served as a negative control. A band corresponding to the expected size of the ∼3.2 kb dicistronic RNA was detected with a Fluc-specific cDNA probe. No monocistronic RNA species corresponding to monocistronic Fluc mRNA were detectable, making a role for UNR 5′-UTR dependent RNA splicing or cleavage events in the translation of the second cistron very unlikely. Next, by performing a more detailed semi-quantitative analysis, we further ruled out the possibility of Fluc expression being a result from translation of a mRNA cleavage product. Therefore, we prepared in parallel with the poly A$^+$ mRNA also protein extracts from the HEK293T transfectants (Di-pRF-UNR and Mono-Fluc/Mono-Rluc). It should be noted that the transfection efficiencies were comparable, as monitored by Rluc activities (data not shown). We made a serial dilution (1/2) starting from 10 μg down to 1.25 μg protein of a cell extract from the mono-Fluc transfectants, and monitored Fluc protein expression by western blot analysis using anti-Fluc antibodies. From the di-pRF-UNR transfectants, a 10 μg cell extract was loaded (Figure 2C, lower panel). The Fluc expression level monitored in the di-pRF-UNR

transfected cell extracts corresponds to the signal obtained with the 2.5 μg mono-Fluc cell extract. This is in agreement with our previous observation that the 3′ cistron (Fluc) on the Di-pRF-UNR mRNA is translated with a ±20% efficiency compared with the monocistronic Fluc control (Figure 1C). If the Fluc protein expression by di-pRF-UNR resulted from a cleaved dicistronic mRNA species, we should be able to see it on the northern blot, as the expected signal of such a band should be of a similar intensity to that of the band detected in the 0.25 μg RNA extract from the monocistronic control (Figure 2C, upper panel, lane 4). As we cannot detect such a band in the Di-pRF-UNR expressing cells (Figure 2C, upper panel, lane 1), it can be ruled out that a monocistronic mRNA species is responsible for Fluc protein expression in the Di-pRF-UNR transfectants.

PTB binds to the polypyrimidine tract sequence in the UNR 5′-UTR

In an attempt to identify potential cellular proteins that specifically interact with the UNR 5′-UTR, we surveyed the corresponding RNA sequence for the presence of ITAF consensus binding sites. This revealed two pyrimidine-rich sequences localized at nucleotides 257–270 and nucleotides 335–355 of the human UNR 5′-UTR that are potential binding sites for the cellular RNA binding pyrimidine tract binding protein PTB (Figure 1A) (36). To examine whether PTB interacts with the UNR 5′-UTR, UV cross-linking experiments in which radiolabeled UNR 5′-UTR RNA was incubated with recombinant His-tagged PTB (a gift from Dr J. Jackson) were performed. EMCV IRES RNA and PITSLRE IRES RNA served as a positive and a negative control, respectively. The EMCV IRES RNA is known for its strong interaction with PTB (37). The PITSLRE RNA is devoid of pyrimidine-rich sequences and does not bind PTB (S. Tinton, unpublished results). Figure 3A clearly illustrates the binding of His-tagged PTB to the UNR 5′-UTR and EMCV IRES probes. The specificity of the interaction between the UNR RNA and PTB was also determined by performing UV cross-linking reactions in the presence of excess unlabeled UNR RNA, EMCV RNA or PITSLRE RNA. PTB binding was successfully prevented by molar excess of unlabeled UNR RNA or EMCV IRES RNA, whereas an excess of PITSLRE IRES RNA had no effect on the binding, indicating that recombinant PTB interacts specifically with the UNR 5′-UTR.

We next investigated whether the UNR 5′-UTR interacts with the PTB protein present in cell extracts. Radiolabeled UNR 5′-UTR or EMCV IRES probes were mixed with cell lysates derived from parental HEK293T cells or from HEK293T cells overexpressing E-tagged PTB (PTB-E), UV cross-linked and analyzed by SDS–PAGE. The EMCV probe served as a positive control. The results illustrated that a ^{32}P-labeled protein of 58 kDa, corresponding to the size of PTB, is cross-linked with the UNR and EMCV IRES probes (Figure 3B, left panel). This 58 kDa band is most prominent in the UV reactions with the PTB-overexpressing HEK293T cell extracts. To confirm the identity of this band, UV cross-linked complexes were immunoprecipitated with anti-E-tag antibody, which specifically revealed the binding of E-tagged PTB to the UNR 5′-UTR and EMCV IRES probes (Figure 3B, right panel). In all probability, the 58 kDa band detected in the reaction with parental HEK293T cell extracts corresponds to the endogenous PTB protein (Figure 3B, left panel, lane 1). The interaction with the endogenous PTB protein was further confirmed by an RNA affinity chromatography assay. Biotinylated UNR 5′-UTR, EMCV IRES and PITSLRE IRES RNAs bound to streptavidin–agarose beads were incubated with cytosolic extract from HEK293T cells. After extensive washing, RNA bound proteins were eluted from the beads and analyzed by western blotting with anti-PTB antibodies. Figure 3C illustrates that endogenous PTB is present in the eluates of the UNR- and EMCV-beads, but is not detectable in the eluate of the PITSLRE beads, further confirming the specific interaction beween PTB and the UNR 5′-UTR RNA.

In order to map the PTB binding site within the UNR 5′-UTR, a series of deletion mutants were generated (Figure 4A), and their ability to bind PTB was determined by UV cross-linking. Radiolabeled RNAs were mixed with HEK293T cell lysates expressing E-tagged PTB, UV cross-linked and immunoprecipitated with the anti-E-tag antibody. The immunoprecipitated complexes were analyzed by SDS–PAGE. Comparison of the ability of different UNR 5′-UTR mutants to bind PTB illustrates impairment of PTB labeling of probes UNR(1–261) and UNR(1–334). In contrast, a radioactive PTB band was clearly detectable in the reactions with the UNR WT and UNR(1–390) probes, indicating that the region at nucleotides 335–390 contributes to the PTB binding site. To examine whether the second pyrimidine-rich stretch located at nucleotides 335–355 is involved in the interaction with PTB, we generated a deletion mutant (UNRΔ335–355) lacking this sequence. As illustrated in Figure 4C, this deletion was associated with a significant decrease in PTB labeling efficiency, indicating that the region spanning nucleotides 335–355 is important for efficient interaction between PTB and UNR 5′-UTR RNA. Similar results were obtained when the binding of endogenous PTB to the different UNR 5′-UTR mutants was analyzed (Figure 4D).

PTB suppresses UNR IRES-driven protein expression

To investigate the role of PTB in UNR 5′-UTR-mediated initiation of translation, we cotransfected the dicistronic reporter plasmid di-pRF-UNR with a plasmid expressing PTB or a mutant of PTB lacking the nuclear localization sequence (PTBΔnls) in three different cell lines: CHO, Cos-1 and HEK293T. PTBΔnls is expressed exclusively in the cytoplasm, whereas the full-length PTB protein resides in the nucleus and the cytoplasm (data not shown). The use of the PTBΔnls mutant therefore excludes involvement of nuclear regulation mechanisms. In each cell line, overexpression of PTB or PTBΔnls induced a 2- to 4-fold decrease in Fluc activity, whereas Rluc activity remained constant (Figure 5A). Western blot analysis of HEK293T cell lysates with anti-PTB antibody indicates that PTB transfection significantly increases the overall PTB protein expression level (Figure 5B; anti-PTB antibody was raised against an N-terminal peptide and therefore does not recognize the PTBΔnls mutant). Further immunoblotting experiments also demonstrated that the decreased Fluc activity measured in cells overexpressing PTB or PTBΔnls is due to lower Fluc protein expression levels (Figure 5B). Consistently, the

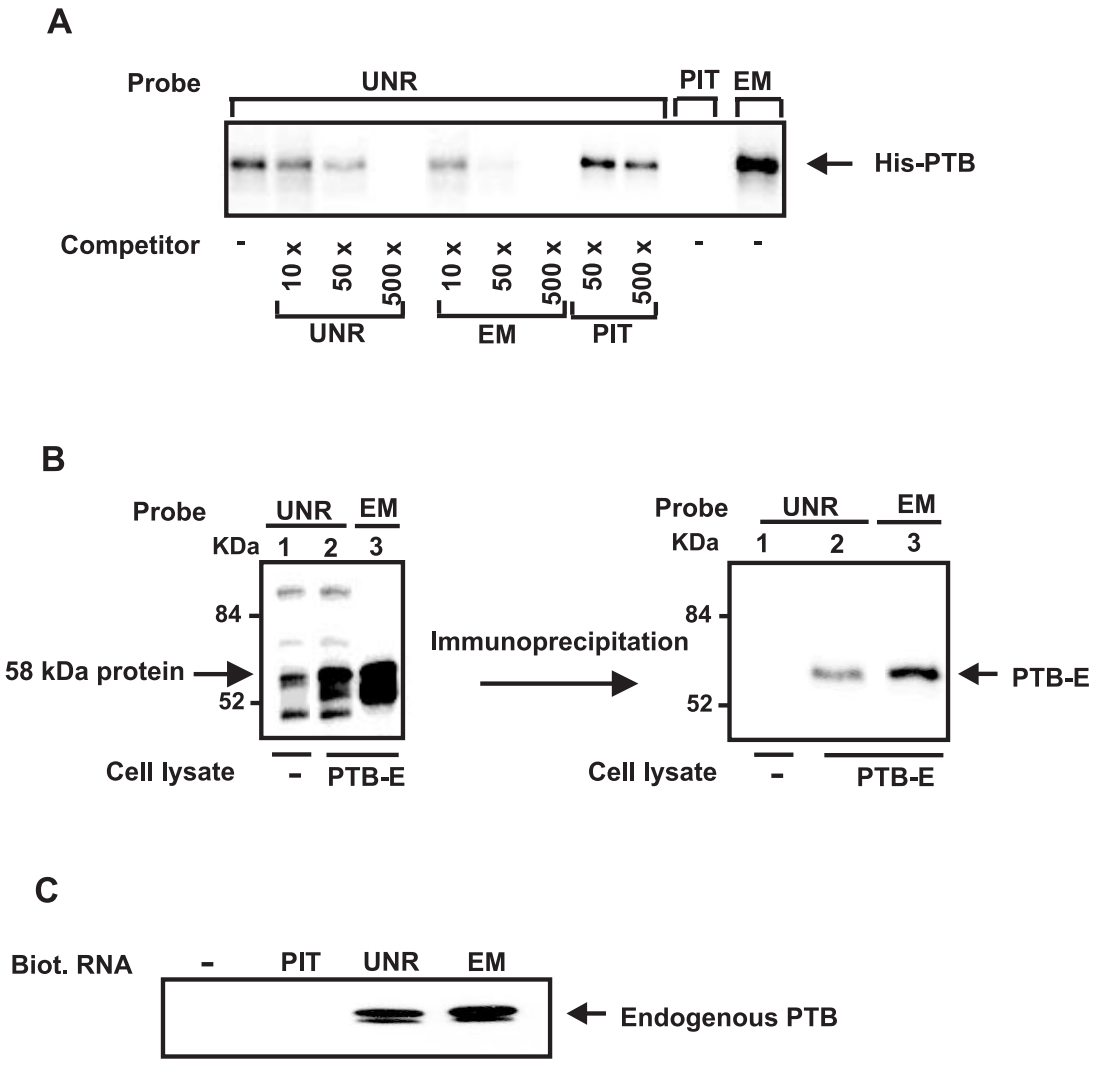

Figure 3. PTB interacts with the UNR 5′-UTR. (**A**) Recombinant His-tagged PTB protein interacts with the UNR 5′-UTR. UV cross-linking assays were performed by pre-incubating 400 ng of His-tagged PTB protein with ^{32}P-labeled probes corresponding to the UNR 5′-UTR, the EMCV IRES (EM) or the PITSLRE IRES (PIT), as indicated. In the case of the UNR 5′-UTR, specificity was determined by prior incubation of the UNR 5′-UTR probe in the absence or presence of 10–500 molar excess of unlabeled UNR IRES transcript, EMCV IRES transcript (EM) or PITSLRE IRES transcript (PIT), respectively. After RNA binding and UV-irradiation, samples were treated with an RNase cocktail and resolved by SDS–PAGE. The arrow depicts the position of cross-linked His-tagged PTB. (**B**) Cytoplasmic extracts from parental HEK293T cells (−) or from HEK293T cells overexpressing E-tagged PTB (PTB-E) were prepared as described in Materials and Methods. After incubation and UV-irradiation with the RNA probes corresponding to the UNR 5′-UTR or the EMCV IRES (EM), samples were treated with an RNase cocktail. One part of the sample was analyzed by SDS–PAGE (left panel), the other part was further mixed with anti-E-tag antibody for immunoprecipitation of labeled E-tagged PTB. Bound proteins were analyzed by SDS–PAGE. The arrow depicts the position of cross-linked E-tagged PTB (right panel). (**C**) Biotinylated UNR, EMCV (EM) and PITSLRE (PIT) IRES RNAs bound to streptavidin beads were incubated with cytoplasmic extracts from parental HEK293T cells as described in Materials and Methods. After extensive washing, RNA bound proteins were analyzed by western blotting using anti-PTB antibodies. The arrow depicts the position of endogenous PTB.

endogenous UNR protein expression level in HEK293T cells transfected with PTB or PTBΔnls was also decreased compared with that in control cells (Figure 5B). Northern blot analysis illustrated that PTB-induced downregulation of Unr protein expression was not due to lower UNR mRNA expression levels. The presence of three UNR mRNA species reflects the use of an alternative polyadenylation signal (23,38). All together, these results suggest that PTB suppresses UNR protein expression by inhibiting UNR IRES-mediated translation.

To further confirm the negative function of PTB on UNR IRES activity, we evaluated UNR IRES activity in HEK293T cells treated with PTB siRNA. If PTB negatively regulates the UNR IRES, one would expect that knockdown of PTB enhances the activity of the UNR IRES. Transfection of PTB siRNA into HEK293T cells, but not of a nonspecific siRNA (NT siRNA), resulted in a strong reduction of endogenous PTB levels (Figure 6). Expression of the unrelated β-actin protein was also analyzed and shown to remain unchanged, indicating the specificity of the PTB siRNA. siRNA-mediated knockdown of PTB led to a 2-fold increase of UNR IRES activity. This effect was not seen with unrelated siRNA. All together, these results indicate again that PTB impacts negatively on the UNR IRES.

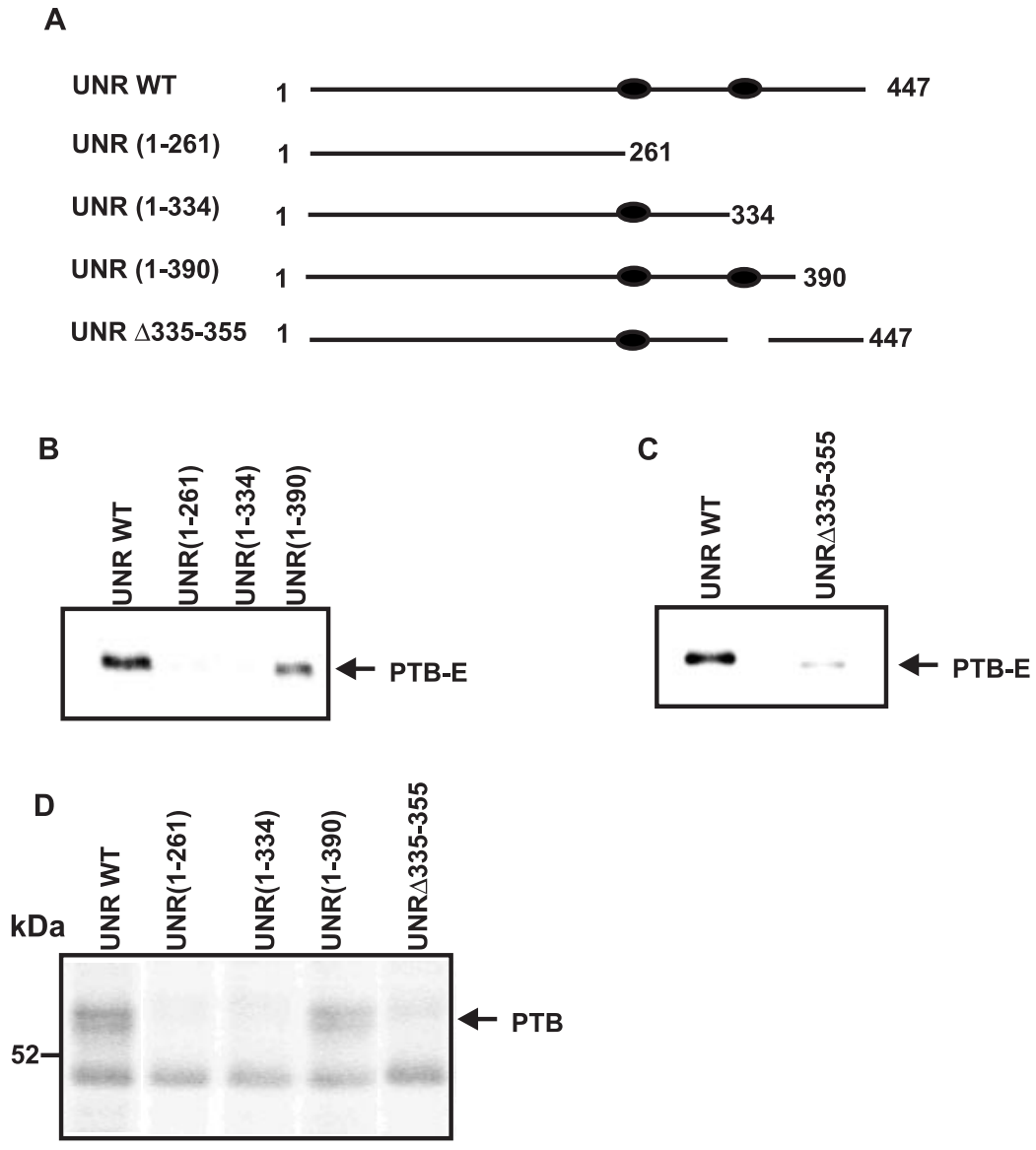

Figure 4. Deletion of the second pyrimidine-rich sequence in the UNR 5′-UTR RNA strongly reduces its binding to PTB. (**A**) Schematic representation of the UNR 5′-UTR fragments used in UV cross-linking reactions. Numbers indicate the positions of the nucleotides based on the human UNR cDNA. The black ellipses represent the CU-rich regions at positions (257–270) and (335–355) in the UNR 5′-UTR element. (**B** and **C**) UV cross-linking of ^{32}P-labeled UNR fragments with cell extracts derived from HEK293T cells overexpressing PTB-E, followed by immunoprecipitation of labeled E-tagged PTB and SDS–PAGE. (**D**) UV cross-linking of ^{32}P-labeled UNR fragments with HEK293T cell extracts, followed by SDS–PAGE. The arrow indicates the position of endogenous PTB.

Deletion of the polypyrimidine tract enhances the basal IRES activity

To determine whether the PTB-induced decrease in IRES-mediated translation of UNR is mediated by the binding of PTB to the polypyrimidine tract in the UNR 5′-UTR, a deletion mutant of the UNR 5′-UTR lacking the PTB binding sequence (UNR 5′-UTRΔ335–355) was analyzed for its ability to drive IRES-mediated translation in a dicistronic reporter assay (Figure 7A). UNR 5′-UTRΔ335–355 was twice as effective as the full-length UNR 5′-UTR in mediating internal initiation of translation, indicating that nucleotides 335–355 have an inhibitory effect on UNR IRES-mediated translation. Furthermore, the inhibitory effect of overexpression of PTB was diminished in mutant UNR 5′-UTRΔ335–355, again indicating an important role for this region in PTB binding (Figure 7A).

We wanted to exclude the possibility that the increased IRES activity mediated by the UNRΔ335–355 deletion mutant was due to a cryptic promoter that could, for example, be activated by deletion of an inhibitory sequence. We therefore tested the effect of transfection of HEK293T cells with pGL3-UNRΔ335–355, in which the UNR 5′-UTR lacking nucleotides 335–355 was inserted in the promoterless pGL3-basic vector upstream of the Fluc coding sequence. PGL3-SV40 served as a positive control. Cells were cotransfected with pSV-Sport *Renilla* luciferase to correct for variation in transfection efficiency. Relative Fluc activity measured in pGL3-UNRΔ335–355 transfected cells was not significantly higher than that in

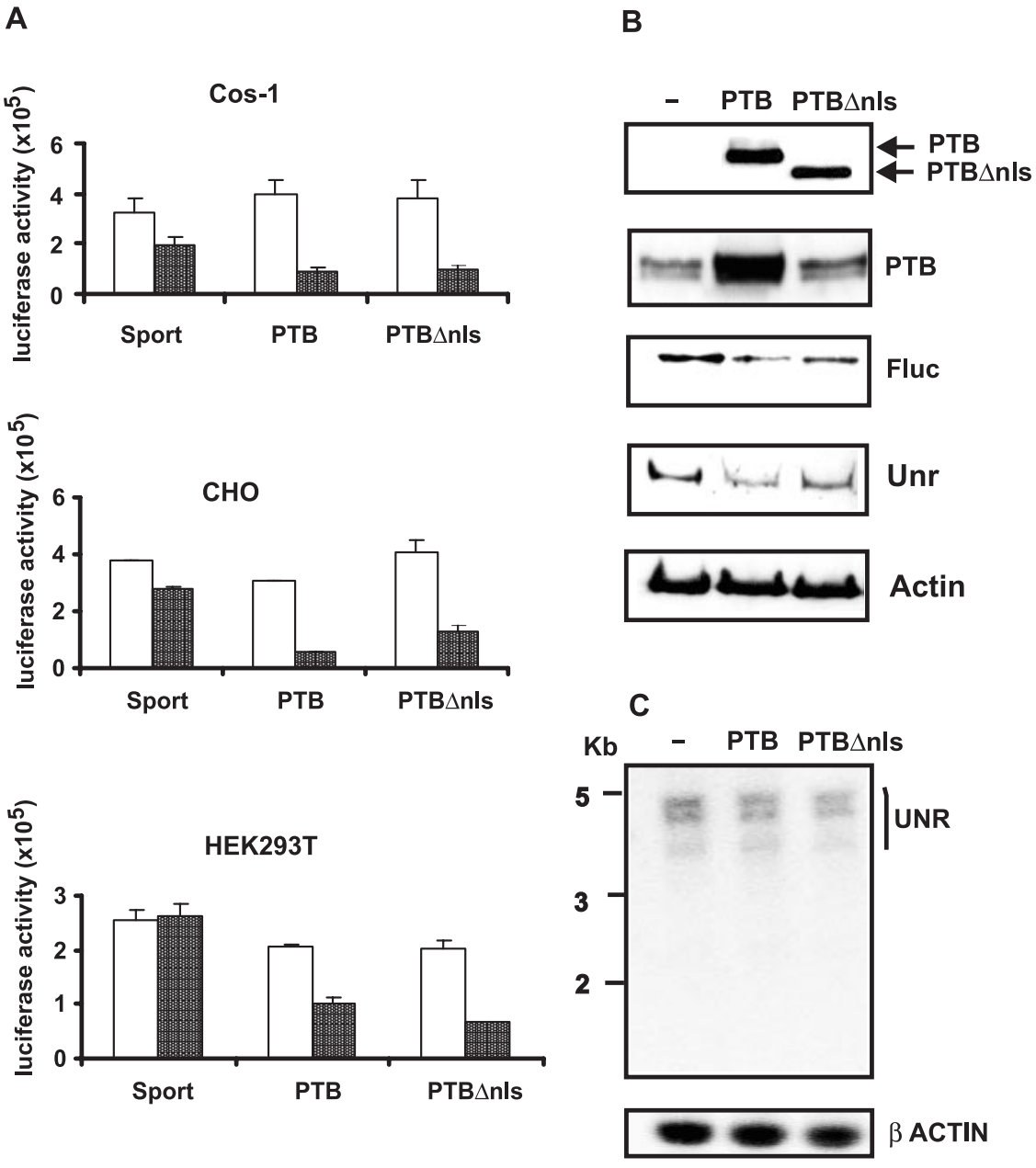

Figure 5. PTB overexpression inhibits IRES-mediated translation of UNR in cultured cells. (**A**) Effect of PTB on UNR IRES-driven expression in a dicistronic reporter assay. Cos-1, CHO and HEK293T cells were cotransfected with the dicistronic reporter plasmid, Di-pRF-UNR and the expression plasmid for PTB or PTBΔnls. Fluc and Rluc activities were measured in the corresponding cell extracts 24 h later. The bars represent the average activities ($n = 3$) ± SD of Fluc (hatched bars) and Rluc (open bars). Bars are representative of three independent experiments. (**B**) Overexpression of PTB suppresses Unr protein expression. Cell lysates from HEK293T cells cotransfected with Di-pRF-UNR and PTB or PTBΔnls were analyzed for PTB, Fluc or Unr protein expression by western blotting and detection with anti-PTB anti-E-tag, anti-Fluc or anti-Unr antibodies, respectively. β-Actin expression levels were analyzed as a loading control. (**C**) Overexpression of PTB has no effect on UNR mRNA levels as revealed by northern blotting. A cDNA corresponding to the *unr* open reading frame was used as a probe. Detection of β-actin mRNA levels served as a loading control. Numbers on the left indicate the length of RNA markers (New England Biolabs).

pGL3-UNR transfected cells, excluding the presence of cryptic promoter activity in the UNR 5′-UTR (Figure 7B).

DISCUSSION

In the present paper we provide evidence that the transcript leader of UNR mRNA contains an IRES. We made use of the well-known dicistronic vector approach. As this approach is conclusive for IRES function only if additional criteria are considered (3), we performed several control experiments that excluded any contribution of a cryptic promoter or RNA processing events to the ability of the UNR 5′-UTR to direct translation of the downstream gene on the dicistronic messenger. Moreover, we also showed that the dicistronic reporter transcript synthesized *in vitro* was able to direct cap-dependent as well as IRES-dependent translation in an

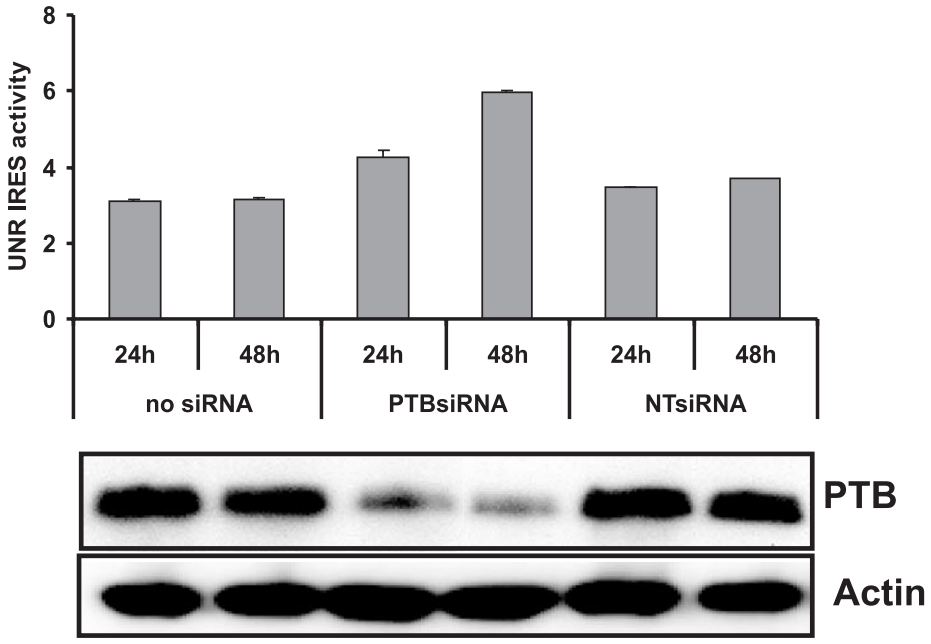

Figure 6. RNAi-mediated depletion of PTB in HEK293T cells stimulates UNR IRES activity. Di-pRF-UNR was transfected in HEK293T cells treated with PTB siRNA as described in Materials and Methods. Cells were analyzed 24 and 48 h after the last siRNA transfection for UNR IRES activity by measuring Rluc and Fluc activities, which are expressed as a ratio of Fluc to Rluc ($n = 2$) ± SD. Bars are representative of two independent experiments. Western blot analysis of HEK293T cells treated with PTB siRNA or with a nonspecific RNAi duplex (NT siRNA) revealed that PTB expression was strongly reduced upon PTB siRNA transfection. Actin was used as an internal control.

in vitro translation assay. As these *in vitro* assays require the use of the dicistronic transcripts themselves instead of the dicistronic plasmids, contribution of any cryptic promoter sequence or splicing event in the translation of the second cistron can be definitively ruled out, confirming the existence of IRES activity in the UNR 5′-UTR.

One can speculate on the physiological role of the UNR IRES. Unr is required for translation from the human rhinovirus-2 (HRV-2) and polio IRES (21,32). Unr has also been described as an ITAF for several cellular IRESes (19,22). Consequently, persistent expression of the cellular Unr protein is needed for translation of certain viral and cellular RNAs under conditions of reduced cap-dependent translation, such as viral infection, apoptosis, mitosis or other cellular stress conditions. Under these conditions, the IRES can serve to sustain Unr synthesis in a cap-independent manner.

We have previously reported that Unr expression levels oscillate during cell cycle progression, from low at the G1 stage to optimal at the G2/M stage (22), suggesting the existence of regulatory mechanisms that tightly control Unr protein expression levels. Here we found that PTB can act as a negative regulator of UNR IRES-mediated translation by specifically interacting with a pyrimidine-rich region (nucleotides 335–355) within the UNR 5′-UTR. Consistently, a UNR IRES mutant lacking the PTB binding site showed increased IRES activity compared to that of the wild-type message, confirming the suppressive role of the nucleotides 335–355 sequence, probably due to its interaction with PTB. However, the observations that PTB binding and the inhibitory effect of the overexpression of PTB on UNR IRES activity were not completely lost in the deletion mutant UNR 5′-UTRΔ335–355 suggest that, in addition to the nucleotides 335–355 sequence, other sequences present in the UNR 5′-UTR could also participate in the PTB interaction with the UNR IRES. This was further confirmed by the observation that the UNR IRES deletion mutants UNR(261–446) and UNR(335–446), which still contain the pyrimidine-rich stretch located at nucleotides 335–355, were able to bind the PTB protein although with reduced affinity compared with the full-length UNR IRES (data not shown). PTB contains four RNA recognition motifs, and the binding of PTB to viral IRESes is consistent with the notion that this protein interacts with several structures to bring the IRES into the correct conformation for ribosome binding. How PTB downregulates internal initiation on the UNR mRNA is still unclear. PTB interaction with the UNR RNA could obstruct the binding of some ITAFs by steric hindrance or by competing for the same binding site. PTB binding could also impact the conformational state of the IRES element, blocking the binding of some stimulatory ITAFs. hnRNPC1/C2 and La autoantigen, which have already been described as ITAFs for XIAP and c-*myc* IRESes (39,40), and the XIAP and BiP IRESes (41,42), respectively, have a high affinity for pyrimidine-rich and poly(U)-rich sequences (43,44). A possible role for these ITAFs in UNR IRES-mediated translation awaits further experiments.

What is the physiological role of the inhibition of UNR mRNA translation by PTB? In this context it is interesting to note that constitutive overexpression of Unr protein in pre-B Ba/F3 cells renders these transfectants much more sensitive to cell death (S. Cornelis, unpublished results), suggesting that a constitutive high expression level of the Unr protein in the cell becomes cytotoxic. So it is tempting to speculate that PTB

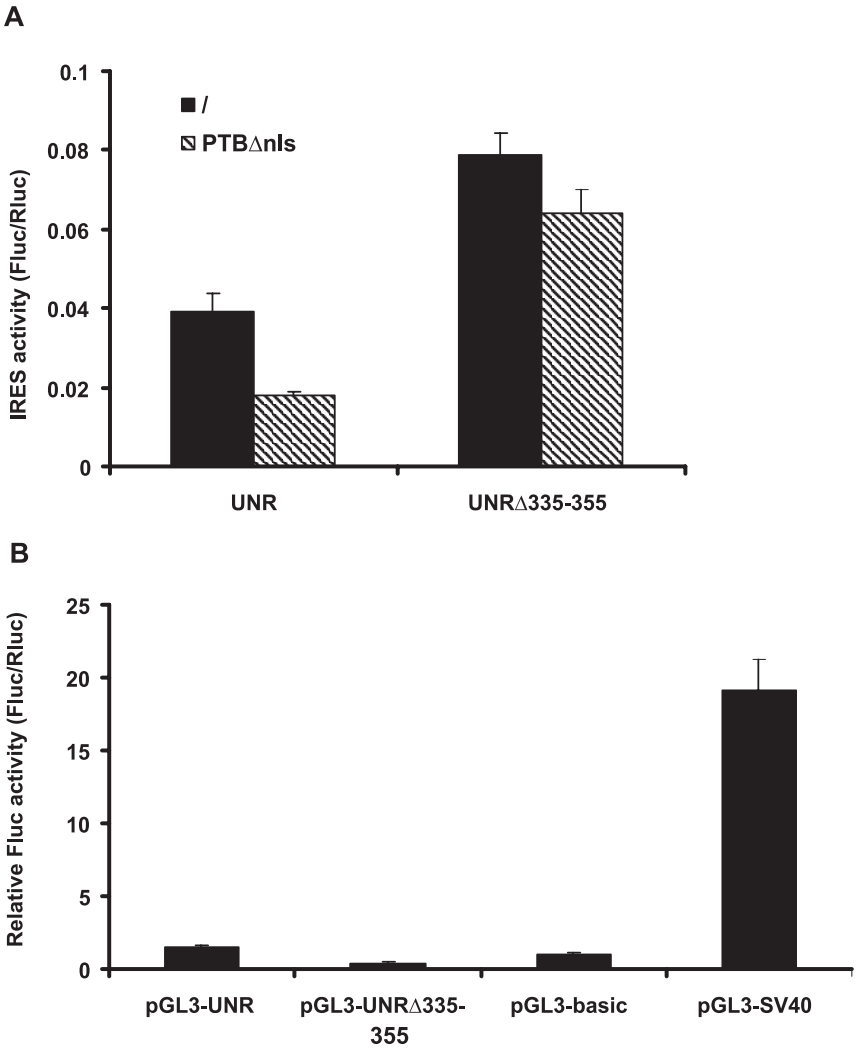

Figure 7. Deletion of a PTB binding site in the UNR 5′-UTR enhances UNR IRES activity. (**A**) The dicistronic expression vectors Di-pRF-UNR and Di-pRF-UNRΔ355–375 were cotransfected in HEK293Tcells with the empty pCAGGS vector or with one containing PTBΔnls. Cells were analyzed 24 h later for Rluc and Fluc activities, which are expressed as a ratio of Fluc to Rluc ($n = 3$) ± SD. Bars are representative of three independent experiments. (**B**) Investigation of potential cryptic promoter activity present in the UNR 5′-UTRΔ335–355 mutant. pGL3-UNR, pGL3-UNRΔ335–355, pGL3-SV40 and pGL3-basic were cotransfected with the pSV-Sport *Renilla* luciferase plasmid in HEK293T cells. Bars represent the average ($n = 3$) ± SD of the ratio between the Fluc and Rluc activities. Bars are representative of three independent experiments.

binding to the UNR IRES keeps translation of this mRNA at a low level in resting or un-stimulated cells. Only under specific conditions, when higher Unr protein expression levels are needed, might bound PTB dissociate from the UNR RNA owing to direct competition from stimulatory ITAFs, or by changes in the conformational state of the UNR RNA induced by interactions with other RNA binding proteins.

Our data indicate that cell signaling pathways altering the binding of PTB to the UNR RNA can influence Unr protein expression. Given the important role of Unr in IRES-dependent translation of various viral and cellular mRNAs, exploring the effects of upstream regulatory molecules on PTB function, as well as the further identification of ITAFs involved in UNR IRES-mediated translation, will definitely lead to a better understanding of the regulation of cap-independent translation.

ACKNOWLEDGEMENTS

This work was supported by grants from the Belgische Federatie tegen Kanker, the Interuniversitaire Attractiepolen, and the Fonds voor Wetenschappelijk Onderzoek-Vlaanderen (FWO). B.S. is a predoctoral research fellow with the Vlaams Instituut voor de Bevordering van het Wetenschappelijk-technologisch Onderzoek in de Industrie. S.C. is a postdoctoral research associate with the FWO. We thank Dr R. Jackson (Department of Biochemistry, University of Cambridge, UK) for providing anti-Unr antisera and recombinant PTB. We are grateful to Dr Amin Bredan for critical reading of the manuscript, and to A. Meeuws and W. Burm for their technical assistance. Funding to pay the Open Access publication charges for this article was provided by the University of Ghent.

Conflict of interest statement. None declared.

REFERENCES

1. Pestova,T.V., Kolupaeva,V.G., Lomakin,I.B., Pilipenko,E.V., Shatsky,I.N., Agol,V.I. and Hellen,C.U. (2001) Molecular mechanisms of translation initiation in eukaryotes. *Proc. Natl Acad. Sci. USA*, **98**, 7029–7036.
2. Stoneley,M. and Willis,A.E. (2004) Cellular internal ribosome entry segments: structures, trans-acting factors and regulation of gene expression. *Oncogene*, **23**, 3200–3207.
3. Vagner,S., Galy,B. and Pyronnet,S. (2001) Irresistible IRES. Attracting the translation machinery to internal ribosome entry sites. *EMBO Rep.*, **2**, 893–898.
4. Fernandez,J., Yaman,I., Mishra,R., Merrick,W.C., Snider,M.D., Lamers,W.H. and Hatzoglou,M. (2001) Internal ribosome entry site-mediated translation of a mammalian mRNA is regulated by amino acid availability. *J. Biol. Chem.*, **276**, 12285–12291.
5. Henis-Korenblit,S., Strumpf,N.L., Goldstaub,D. and Kimchi,A. (2000) A novel form of DAP5 protein accumulates in apoptotic cells as a result of caspase cleavage and internal ribosome entry site-mediated translation. *Mol. Cell. Biol.*, **20**, 496–506.
6. Holcik,M., Yeh,C., Korneluk,R.G. and Chow,T. (2000) Translational upregulation of X-linked inhibitor of apoptosis (XIAP) increases resistance to radiation induced cell death. *Oncogene*, **19**, 4174–4177.
7. Morrish,B.C. and Rumsby,M.G. (2002) The 5′ untranslated region of protein kinase Cdelta directs translation by an internal ribosome entry segment that is most active in densely growing cells and during apoptosis. *Mol. Cell. Biol.*, **22**, 6089–6099.
8. Stoneley,M., Chappell,S.A., Jopling,C.L., Dickens,M., MacFarlane,M. and Willis,A.E. (2000) c-Myc protein synthesis is initiated from the internal ribosome entry segment during apoptosis. *Mol. Cell. Biol.*, **20**, 1162–1169.
9. Lang,K.J., Kappel,A. and Goodall,G.J. (2002) Hypoxia-inducible factor-1alpha mRNA contains an internal ribosome entry site that allows efficient translation during normoxia and hypoxia. *Mol. Biol. Cell*, **13**, 1792–1801.
10. Stein,I., Itin,A., Einat,P., Skaliter,R., Grossman,Z. and Keshet,E. (1998) Translation of vascular endothelial growth factor mRNA by internal ribosome entry: implications for translation under hypoxia. *Mol. Cell. Biol.*, **18**, 3112–3119.
11. Coldwell,M.J., de Schoolmeester,M.L., Fraser,G.A., Pickering,B.M., Packham,G. and Willis,A.E. (2001) The p36 isoform of BAG-1 is translated by internal ribosome entry following heat shock. *Oncogene*, **20**, 4095–4100.
12. Brasey,A., Lopez-Lastra,M., Ohlmann,T., Beerens,N., Berkhout,B., Darlix,J.L. and Sonenberg,N. (2003) The leader of human immunodeficiency virus type 1 genomic RNA harbors an internal ribosome entry segment that is active during the G2/M phase of the cell cycle. *J. Virol.*, **77**, 3939–3949.
13. Cornelis,S., Bruynooghe,Y., Denecker,G., Van Huffel,S., Tinton,S. and Beyaert,R. (2000) Identification and characterization of a novel cell cycle-regulated internal ribosome entry site. *Mol. Cell*, **5**, 597–605.
14. Honda,M., Kaneko,S., Matsushita,E., Kobayashi,K., Abell,G.A. and Lemon,S.M. (2000) Cell cycle regulation of hepatitis C virus internal ribosomal entry site-directed translation. *Gastroenterology*, **118**, 152–162.
15. Maier,D., Nagel,A.C. and Preiss,A. (2002) Two isoforms of the Notch antagonist Hairless are produced by differential translation initiation. *Proc. Natl Acad. Sci. USA*, **99**, 15480–15485.
16. Pyronnet,S., Pradayrol,L. and Sonenberg,N. (2000) A cell cycle-dependent internal ribosome entry site. *Mol. Cell*, **5**, 607–616.
17. Qin,X. and Sarnow,P. (2004) Preferential translation of internal ribosome entry site-containing mRNAs during the mitotic cycle in mammalian cells. *J. Biol. Chem.*, **279**, 13721–13728.
18. Zhang,X., Richie,C. and Legerski,R.J. (2002) Translation of hSNM1 is mediated by an internal ribosome entry site that upregulates expression during mitosis. *DNA Repair (Amst)*, **1**, 379–390.
19. Mitchell,S.A., Spriggs,K.A., Coldwell,M.J., Jackson,R.J. and Willis,A.E. (2003) The Apaf-1 internal ribosome entry segment attains the correct structural conformation for function via interactions with PTB and unr. *Mol. Cell*, **11**, 757–771.
20. Pickering,B.M., Mitchell,S.A., Spriggs,K.A., Stoneley,M. and Willis,A.E. (2004) Bag-1 internal ribosome entry segment activity is promoted by structural changes mediated by poly(rC) binding protein 1 and recruitment of polypyrimidine tract binding protein 1. *Mol. Cell. Biol.*, **24**, 5595–5605.
21. Hunt,S.L., Hsuan,J.J., Totty,N. and Jackson,R.J. (1999) unr, a cellular cytoplasmic RNA-binding protein with five cold-shock domains, is required for internal initiation of translation of human rhinovirus RNA. *Genes Dev.*, **13**, 437–448.
22. Tinton,S.A., Schepens,B., Bruynooghe,Y., Beyaert,R. and Cornelis,S. (2005) Regulation of the cell cycle-dependent PITSLRE internal ribosome entry site: roles of upstream of N-ras and phosphorylated translation initiation factor eIF-2alpha. *Biochem. J.*, **385**, 155–163.
23. Doniger,J., Landsman,D., Gonda,M.A. and Wistow,G. (1992) The product of unr, the highly conserved gene upstream of N-ras, contains multiple repeats similar to the cold-shock domain (CSD), a putative DNA-binding motif. *New Biol.*, **4**, 389–395.
24. Jacquemin-Sablon,H., Triqueneaux,G., Deschamps,S., le Maire,M., Doniger,J. and Dautry,F. (1994) Nucleic acid binding and intracellular localization of unr, a protein with five cold shock domains. *Nucleic Acids Res.*, **22**, 2643–2650.
25. Landsman,D. (1992) RNP-1, an RNA-binding motif is conserved in the DNA-binding cold shock domain. *Nucleic Acids Res.*, **20**, 2861–2864.
26. Graumann,P.L. and Marahiel,M.A. (1998) A superfamily of proteins that contain the cold-shock domain. *Trends Biochem. Sci.*, **23**, 286–290.
27. Wolffe,A.P. (1994) Structural and functional properties of the evolutionarily ancient Y-box family of nucleic acid binding proteins. *Bioessays*, **16**, 245–251.
28. Wolffe,A.P., Tafuri,S., Ranjan,M. and Familari,M. (1992) The Y-box factors: a family of nucleic acid binding proteins conserved from *Escherichia coli* to man. *New Biol.*, **4**, 290–298.
29. Sommerville,J. (1999) Activities of cold-shock domain proteins in translation control. *Bioessays*, **21**, 319–325.
30. Capowski,E., Esnault,E.S., Bhattacharya,S. and Malter,J.S. (2001) Y box-binding factor promotes eosinophil survival by stabilizing granulocyte-macrophage colony-stimulating factor mRNA. *J. Immunol.*, **167**, 5970–5976.
31. Chen,Y., Carpenter,S.L. and Lamont,S.J. (2000) A functional role for the Y box in regulating an MHC class II B gene promoter in chicken lymphocytes. *Immunogenetics*, **51**, 882–886.
32. Boussadia,O., Niepmann,M., Creancier,L., Prats,A.C., Dautry,F. and Jacquemin-Sablon,H. (2003) Unr is required *in vivo* for efficient initiation of translation from the internal ribosome entry sites of both rhinovirus and poliovirus. *J. Virol.*, **77**, 3353–3359.
33. O'Mahoney,J.V. and Adams,T.E. (1994) Optimization of experimental variables influencing reporter gene expression in hepatoma cells following calcium phosphate transfection. *DNA Cell Biol.*, **13**, 1227–1232.
34. Bergamini,G., Preiss,T. and Hentze,M.W. (2000) Picornavirus IRESes and the poly(A) tail jointly promote cap-independent translation in a mammalian cell-free system. *RNA*, **6**, 1781–1790.
35. Walker,J., de Melo Neto,O. and Standart,N. (1998) Gel retardation and UV-crosslinking assays to detect specific RNA–protein interactions in the 5′ or 3′ UTRs of translationally regulated RNAs. *Methods Mol. Biol.*, **77**, 365–378.
36. Singh,R., Valcarcel,J. and Green,M.R. (1995) Distinct binding specificities and functions of higher eukaryotic polypyrimidine tract-binding proteins. *Science*, **268**, 1173–1176.
37. Jang,S.K. and Wimmer,E. (1990) Cap-independent translation of encephalomyocarditis virus RNA: structural elements of the internal ribosomal entry site and involvement of a cellular 57-kD RNA-binding protein. *Genes Dev.*, **4**, 1560–1572.
38. Jeffers,M., Paciucci,R. and Pellicer,A. (1990) Characterization of unr; a gene closely linked to N-ras. *Nucleic Acids Res.*, **18**, 4891–4899.
39. Holcik,M., Gordon,B.W. and Korneluk,R.G. (2003) The internal ribosome entry site-mediated translation of antiapoptotic protein XIAP is modulated by the heterogeneous nuclear ribonucleoproteins C1 and C2. *Mol. Cell. Biol.*, **23**, 280–288.
40. Kim,J.H., Paek,K.Y., Choi,K., Kim,T.D., Hahm,B., Kim,K.T. and Jang,S.K. (2003) Heterogeneous nuclear ribonucleoprotein C modulates translation of c-myc mRNA in a cell cycle phase-dependent manner. *Mol. Cell. Biol.*, **23**, 708–720.

41. Holcik,M. and Korneluk,R.G. (2000) Functional characterization of the X-linked inhibitor of apoptosis (XIAP) internal ribosome entry site element: role of La autoantigen in XIAP translation. *Mol. Cell. Biol.*, **20**, 4648–4657.
42. Kim,Y.K., Back,S.H., Rho,J., Lee,S.H. and Jang,S.K. (2001) La autoantigen enhances translation of BiP mRNA. *Nucleic Acids Res.*, **29**, 5009–5016.
43. Gorlach,M., Burd,C.G. and Dreyfuss,G. (1994) The determinants of RNA-binding specificity of the heterogeneous nuclear ribonucleoprotein C proteins. *J. Biol. Chem.*, **269**, 23074–23078.
44. Kenan,D.J., Query,C.C. and Keene,J.D. (1991) RNA recognition: towards identifying determinants of specificity. *Trends Biochem. Sci.*, **16**, 214–220.